

Molecular tuning of fast gating in pentameric ligand-gated ion channels

Thomas Grutter^{*†§}, Lia Prado de Carvalho^{*†}, Virginie Dufresne^{*}, Antoine Taly^{*}, Stuart J. Edelstein[¶], and Jean-Pierre Changeux^{*§}

^{*}Laboratoire "Récepteurs et Cognition," Institut Pasteur, 25 Rue du Dr. Roux, 75724 Paris Cedex 15, France; and [¶]Department of Biochemistry, University of Geneva, 30 Quai Ernest-Ansermet, CH-1211 Geneva 4, Switzerland

Contributed by Jean-Pierre Changeux, October 17, 2005

Neurotransmitters such as acetylcholine (ACh) and glycine mediate fast synaptic neurotransmission by activating pentameric ligand-gated ion channels (LGICs). These receptors are allosteric transmembrane proteins that rapidly convert chemical messages into electrical signals. Neurotransmitters activate LGICs by interacting with an extracellular agonist-binding domain (ECD), triggering a tertiary/quaternary conformational change in the protein that results in the fast opening of an ion pore domain (IPD). However, the molecular mechanism that determines the fast opening of LGICs remains elusive. Here, we show by combining whole-cell and single-channel recordings of recombinant chimeras between the ECD of $\alpha 7$ nicotinic receptor (nAChR) and the IPD of the glycine receptor (GlyR) that only two GlyR amino acid residues of loop 7 (Cys-loop) from the ECD and at most five $\alpha 7$ nAChR amino acid residues of the M2-M3 loop (2-3L) from the IPD control the fast activation rates of the $\alpha 7$ /Gly chimera and WT GlyR. Mutual interactions of these residues at a critical pivot point between the agonist-binding site and the ion channel fine-tune the intrinsic opening and closing rates of the receptor through stabilization of the transition state of activation. These data provide a structural basis for the fast opening of pentameric LGICs.

allosteric proteins | chimeric receptor | Cys-loop receptor | transition state

Pentameric ligand-gated ion channels (LGICs), such as the cationic nicotinic acetylcholine receptor (nAChR) and the anionic glycine receptor (GlyR), mediate fast excitatory or inhibitory chemical neurotransmission between neurons (1–6). A unique feature of these receptors is that they activate the ion channel, a process known as gating, in less than a ms. For nicotinic receptors, a detailed single-channel analysis has recently established a speed limit for the opening of the ion channel in the μ s time range (7). Perturbations of this rapid transmission pathway by natural mutants lead to severe diseases such as congenital myasthenic syndromes (8), hereditary hyperekplexia (9), or epileptic disorders (10).

Pentameric LGICs, or Cys-loop receptors, are composed of five homologous subunits, sharing a common structural organization, arranged (pseudo)symmetrically around the central ion pore (1, 2). All subunits are made of two distinct topological domains: the extracellular (ECD) and the ion pore domains (IPD). First, the ECD is folded into a twisted β -sandwich core, as revealed by x-ray crystallographic studies of the mollusk acetylcholine-binding protein (AChBP), a soluble pentameric protein homologous to the extracellular domain of LGICs (11–14). Second, electron microscopy images of *Torpedo* nAChR at 4-Å resolution revealed that the four transmembrane segments (M1 to M4) of the IPD are folded into α -helices joined by linking loops of variable lengths (15). By combining these structural data, we built a 3D model of the full $\alpha 7$ nAChR (16). In this model, the coupling zone located at the interface between the two domains is framed by flexible loops. As noted earlier for GABA_A receptors (17), loops 2 and 7 (the so-called Cys-loop) from the ECD are close (<5 Å) to the C-terminal end of α -helix M2 from the IPD. Even though structural information is now

available for the linking of the ECD and IPD, the molecular mechanism coupling the agonist-binding site and ion channel resulting in the fast opening of the ion channel remains elusive.

In this article, we show, by combining whole-cell and single-channel recordings of recombinant chimeras between the ECD of the homomeric $\alpha 7$ nicotinic receptor (nAChR) and the IPD of the homomeric $\alpha 1$ glycine receptor (GlyR), that only two GlyR amino acid residues of the Cys-loop from the ECD and at most five $\alpha 7$ nAChR amino acid residues of the M2-M3 loop (2–3L) from the IPD fine-tune the fast activation rates of the $\alpha 7$ /Gly chimera and WT GlyR. We propose that mutual interactions of these residues with their WT counterparts in the LGICs result in the acceleration of both the intrinsic opening and closing rate constants through stabilization of the transition state of activation. These data provide a structural basis for the fast opening of pentameric LGICs.

Methods

Mutagenesis. Chick $\alpha 7$ cDNA encoding the ECD of $\alpha 7$ nAChR was fused with the human $\alpha 1$ cDNA encoding the IPD of $\alpha 1$ glycine receptor. Chimeric cDNAs were subcloned into pMT3 containing the peptide signal sequence of the $\alpha 7$ subunit. Mutants of the Cys-loop region were performed on the synthetic gene of the $\alpha 7$ subunit as described (18), whereas, for the 2–3L region and WT GlyR, mutations were created by using the QuikChange kit (Stratagene) according to the manufacturer's instructions. All mutant and chimeric cDNAs were verified by restriction enzyme analysis and sequencing.

Whole-Cell Recordings. Human embryonic kidney cells (HEK 293) were grown and transiently transfected as described (18). Recordings were made 48–72 h after transfection at room temperature (25°C \pm 3°C), by using the whole-cell patch-clamp technique (19). Cells were maintained at a holding potential of –60 mV. External solution contained 140 mM NaCl, 2.8 mM KCl, 2 mM CaCl₂, 2 mM MgCl₂, 10 mM Glucose, and 10 mM Hepes–NaOH (pH 7.3); Ca²⁺ and Mg²⁺ were removed just after the whole-cell configuration was obtained. To determine chloride permeability of the channel, extracellular chloride was reduced through total replacement of NaCl of the external solution by 140 mM sodium isethionate. Patch pipette (1–2 M Ω) solutions contained 140 mM CsCl₂, 2 mM NaATP, 10 mM Hepes–CsOH, and 10 mM EGTA (pH 7.3). Current-voltage relationships were determined by the application of two inverted voltage ramps (+50 to –100 mV in 200 ms, from an initial holding potential of –60 mV) during the steady-state phase of an ACh-evoked

Conflict of interest statement: No conflicts declared.

Abbreviations: LGIC, ligand-gated ion channel; nAChR, nicotinic acetylcholine receptor; GlyR, glycine receptor; ECD, extracellular agonist-binding domain; IPD, ion pore domain; 2–3L, M2-M3 loop.

[†]T.G. and L.P.d.C. contributed equally to this work.

[§]To whom correspondence may be addressed. E-mail: grutter@pasteur.fr or changeux@pasteur.fr.

© 2005 by The National Academy of Sciences of the USA

residues from $\alpha 7$ and IPD residues from GlyR might not be optimal, conferring a poor coupling between the two domains. To test this hypothesis, we replaced in $\alpha 7$ /Gly its chick $\alpha 7$ Cys-loop by the homologous human $\alpha 1$ GlyR Cys-loop. This substitution resulted in a new chimera $\alpha 7(\text{Cys-L})/\text{Gly}$ that displayed enhanced activation rates at saturating concentrations of ACh concomitant with an increase of the apparent desensitization rate (Fig. 2*b*). These data demonstrate that the Cys-loop plays a major role in the fast activation rate in the $\alpha 7(\text{Cys-L})/\text{Gly}$ chimera.

The Cys-Loop Stabilizes the Transition State of Activation. These results might be explained by changes in agonist association rates, channel-gating rates, and/or conductance levels. The following observations support a change in the channel-gating rates only.

First, whole-cell dose-response curves revealed no significant differences of EC_{50} values between $\alpha 7$ /Gly and $\alpha 7(\text{Cys-L})/\text{Gly}$ chimeras (Fig. 2*c*). Furthermore, no differences were noticed in the apparent dissociation constants of ACh as measured by competition against α - ^{125}I -bungarotoxin binding to intact cells (Fig. 2*d*). Second, compared with $\alpha 7$ /Gly, a parallel increase of k_{app} was observed for $\alpha 7(\text{Cys-L})/\text{Gly}$ (Fig. 2*e*). As a result, significant increases in both k_{open} ($16.4 \pm 3.9 \text{ s}^{-1}$) and k_{closed} ($1.77 \pm 0.68 \text{ s}^{-1}$) were observed (7-fold for k_{open} and 9-fold for k_{closed} , $P < 0.01$; for other kinetic details, see *Supporting Materials and Methods*). Third, single-channel recordings revealed that 10 μM ACh elicited shorter openings in $\alpha 7(\text{Cys-L})/\text{Gly}$ as compared with $\alpha 7$ /Gly chimera (Fig. 2*f*). Indeed, open-time histograms were fitted with three exponential components for $\alpha 7(\text{Cys-L})/\text{Gly}$ ($\tau_1 = 0.89 \text{ ms}$, $a_1 = 0.35$; $\tau_2 = 8.5 \text{ ms}$, $a_2 = 0.35$; $\tau_3 = 65 \text{ ms}$, $a_3 = 0.30$) and with four components for $\alpha 7$ /Gly ($\tau_1 = 0.75 \text{ ms}$, $a_1 = 0.20$; $\tau_2 = 5.9 \text{ ms}$, $a_2 = 0.21$; $\tau_3 = 42 \text{ ms}$, $a_3 = 0.28$; $\tau_4 = 193 \text{ ms}$, $a_4 = 0.31$; Fig. 2*g*). A left-shift to shorter open-time values of all components was observed for $\alpha 7(\text{Cys-L})/\text{Gly}$ compared with $\alpha 7$ /Gly that resulted in a 3-fold decrease of the mean open time ($\tau_{\text{mean}} = 23 \text{ ms}$ for $\alpha 7(\text{Cys-L})/\text{Gly}$ versus $\tau_{\text{mean}} = 73 \text{ ms}$ for $\alpha 7$ /Gly). This decrease implies that the shortest component for $\alpha 7(\text{Cys-L})/\text{Gly}$ equivalent to that observed for $\alpha 7$ /Gly is likely to be missed, explaining that only three exponential components were sufficient to fit the data. Because the number of channels in patches is unknown, comparison of the closed time histograms between chimeras was judged to be uninformative and was not included. Fourth, no significant modifications on the conductance levels were observed for both chimeras (data not shown). Finally, to help illustrate the experimental data, a set of theoretical parameters derived from a kinetic-based allosteric model (see Fig. 6, which is published as supporting information on the PNAS web site) (27) simulated adequately the macroscopic currents (Fig. 2*h*) and open-time distribution of $\alpha 7$ /Gly (Fig. 2*g*; for modeling details, see *Supporting Materials and Methods*). It should be noted that these simulations illustrate only the functional results and do not result from a fitting procedure through the data. Simulations show that changing only the intrinsic opening and closing rates in $\alpha 7(\text{Cys-L})/\text{Gly}$ resulted in the expected increase of the activation rate observed in whole-cell recordings (Fig. 2*h*) and decrease of the mean open time observed in single-channel recordings (Fig. 2*g*). In term of free energy, simulations predicted a stabilization of the transition state between the closed and open conformations ($\Delta\Delta G^\ddagger$) by -1.36 kcal/mol (Fig. 2*i*). We concluded from these data that the Cys-loop substitution increases the intrinsic opening and closing rates by stabilization of the transition state, without modifying substantially the ACh binding or the ion conduction properties.

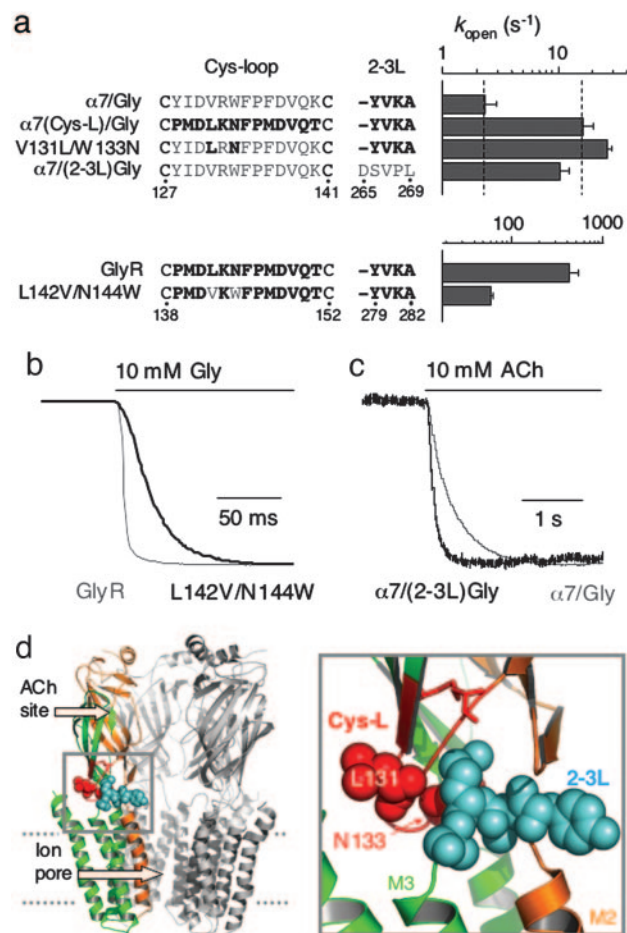


Fig. 3. Tuning the activation kinetics in LGICs. (a) k_{open} bar plot of the indicated constructions. Sequences of the Cys-loop and 2–3L region are indicated. Residues from $\alpha 7$ nAChR are indicated in gray and GlyR in bold-type characters. (b) Normalized whole-cell currents (10 mM glycine) through GlyR WT (gray trace) and L142V/N144W mutant (dark trace). (c) Normalized whole-cell currents (10 mM ACh) through $\alpha 7$ /Gly (gray trace) and $\alpha 7/(2-3\text{L})\text{Gly}$ (dark trace). (d) Mapping of the identified residues on the $\alpha 7$ /Gly 3D model (red spheres for Cys-L and cyan for 2–3L). The inner and outer blocks are colored in orange and green, respectively. For clarity, only four subunits are represented. (Inset) Enlarged view of the coupling zone.

Only Two Residues from the Cys-Loop Fine-Tune the Kinetics of Activation in $\alpha 7$ /Gly and WT GlyR. We next investigated which amino acids within the Cys-loop are responsible for the fast activation rate. A systematic analysis of the Cys-loop was undertaken by introducing microcassettes or single residues of the $\alpha 1$ GlyR Cys-loop into $\alpha 7$ /Gly. For each construction, k_{open} and k_{closed} rates were as previously derived (for a detailed description of each construction, see Fig. 7, which is published as supporting information on the PNAS web site, and *Supporting Materials and Methods*). This study showed that the double mutation V131L/W133N was sufficient to confer a fast activation rate, similar to that of $\alpha 7(\text{Cys-L})/\text{Gly}$ (Fig. 3*a*). Then, to test the reciprocity of the mutation, we produced the converse double mutant L142V/N144W in the WT GlyR. This mutant displayed responses to glycine that were significantly slower (7-fold, $P < 0.05$) than those of the WT GlyR (Fig. 3*a* and *b*). This difference was in the same range (≈ 10 -fold) as observed after the Cys-loop exchange in $\alpha 7$ /Gly chimera (Fig. 3*a*). Consistent with the fact that $\alpha 7(\text{Cys-L})/\text{Gly}$ was not as fast as the WT GlyR, the double mutant L142V/N144W in GlyR remained faster than $\alpha 7$ /Gly chimera (Fig. 3*a*). Overall, our results highlight the functional

importance of the two residues from the Cys-loop in tuning the kinetics of activation in both the chimeric and WT receptors and suggest that other regions from the ECD might also contribute to the fast activation rate.

The M2-M3 Loop also Plays a Major Role in Accelerating the Kinetics of Activation. Finally, the 3D model of $\alpha 7$ /Gly showed that the side chains of the two identified residues of the Cys-loop are in close contact with those of M2-M3 loop (2-3L) (Fig. 3*d*). This loop links the two α -helices M2/M3 and is not conserved between nAChRs and GlyRs/GABA_A receptors (Fig. 5). We reasoned that replacing the human $\alpha 1$ GlyR residues of 2-3L in $\alpha 7$ /Gly (Y279-A282) by the homologous residues of chick $\alpha 7$ nAChR (D265-L269) should restore a homogeneous coupling between the Cys-loop and 2-3L. Therefore, we produced the new chimera $\alpha 7$ /(2-3L)Gly, which indeed displayed a significantly accelerated activation of the current evoked by saturating concentration of ACh, yielding k_{open} values close to those of $\alpha 7$ (Cys-L)/Gly (Fig. 3*a* and *c*). These data show that the introduction of at most five $\alpha 7$ nAChR residues in the 2-3L is sufficient to rescue a homogeneous coupling in $\alpha 7$ /Gly chimera, as did the exchange of two $\alpha 1$ GlyR amino acids in the Cys-loop. Thus, our results demonstrate that both the Cys-loop and the 2-3L region mediate bidirectional allosteric coupling between the agonist-binding and the ion channel domains in LGICs.

Discussion

In the present study, we demonstrate that the Cys-loop and 2-3L region fine-tune the speed of the signal transduction in LGICs. We reached this conclusion by designing a chimeric receptor made from the ECD of $\alpha 7$ nAChR and the IPD of GlyR. This chimera is functional but displays abnormally slow activation rates. By swapping either the Cys-loop or the 2-3L region with their WT counterparts, we succeeded in accelerating the slow activation rate of the $\alpha 7$ /Gly chimera. A mutational analysis indicated that only a double mutation in the Cys-loop (V131L/W133N) suffices to restore the fast activation rate in the chimera. We then succeeded in slowing the WT GlyR by producing the converse double mutant (L142V/N144W). Therefore, the Cys-loop and 2-3L play critical roles in the fine-tuning of fast gating in LGICs. Our results also show that the mutated $\alpha 7$ /Gly chimeras were still not as fast as the WT GlyR and that the mutated GlyR was not as slow as $\alpha 7$ /Gly, suggesting that other regions, yet unidentified (possibly loops 2, 9, and pre-M1, and the C-terminal end of M4), might contribute to the control of the fast gating.

The Cys-loop (28-32) and 2-3L region (17) have been previously identified as important loops for the allosteric coupling; our present work demonstrates their role in the control of the fast opening of the ion channel. Furthermore, sequence analysis shows that the 2-3L region identified here differs from that found earlier in the GABA_A receptor (17). This discrepancy may be explained by local changes in the structure of the 2-3L region in the GABA_A receptor or alternatively by differences in the construction of the 3D model. Indeed, on the basis of the recent EM images of the ion channel, the M2 segment was interpreted as a 40-Å-long α -helix (15), longer than it was commonly assumed. This extension inevitably brings the 2-3L loop to a more C-terminal region that corresponds to the region we identified in the present study.

Our results, supported by the 3D model of the receptor, suggest that the Cys-loop and 2-3L region interact cooperatively to produce fast gating (Fig. 3*d*). Three general conclusions can be drawn about their mutual interactions in the gating process.

First, although a common activation mechanism is shared by cationic and anionic LGICs, fine structural complementarity at the interface region is likely to be a general rule for optimal

allosteric coupling, as already suggested by chimeras made from the acetylcholine-binding protein (AChBP) and the 5HT₃ receptor (18, 32). Indeed, for GlyR coupling, fast gating is mediated by only two nonconserved amino acid residues from the Cys-loop whereas for $\alpha 7$ nAChR fast coupling occurs through at most five nonconserved residues from the 2-3L region. Therefore, optimal coupling in LGICs is mediated by specific interactions, which depend on residues found specifically in anionic versus cationic receptors. The specific coupling interactions between GlyR residues depicted in Fig. 3*d* should therefore be different from those of $\alpha 7$ nAChR. Further experiments are needed to identify the amino acids from the GlyR 2-3L region that interact with the two Cys-loop residues and the amino acids from the $\alpha 7$ nAChR Cys-loop that interact with the five 2-3L residues, to assign more precisely the minimal cluster of residues that mediate fast gating in the LGICs.

Second, the complementary interaction between the Cys-loop and 2-3L results probably in the stabilization of the transition state of gating. In turn, this stabilization allows the fast opening of the ion channel necessary to mediate fast synaptic neurotransmission. For such large multimeric proteins, subtle changes in the transition state energy barrier (≈ 1.36 kcal/mol) might explain their swiftness of activation. We propose that fast gating of LGICs is thus achieved by the interactions of some critical residues that lower the energy barrier by a few kcal/mol.

Third, the interaction of the Cys-loop with 2-3L region facilitates the physical opening of the ion pore. This last conclusion is supported by several structural gating mechanisms (15, 16, 33). In particular, normal mode analysis recently proposed that the conformational transition that causes the opening of the ion pore is essentially a quaternary twist motion of the protein accompanied by discrete tertiary changes of each subunit (16). These tertiary changes correspond to the relative motions of two rigid blocks (Fig. 3*d*). One of these, the inner block, is essentially composed of the inner β -sheet of the ECD that carries the agonist-binding site and α -helix M2 that frames the ion channel wall (16). Therefore, signal transmission between the agonist-binding site and the ion channel is mediated by the intrinsic concerted movement of the rigid inner block. The two flexible loops, the Cys-loop and 2-3L region, undergo discrete conformational changes, enabling the concerted motions of the two rigid blocks associated with a minimal energy cost, facilitating the rapid twist of all five α -helix M2 necessary to open the ion channel (see Movies 1 and 2, which are published as supporting information on the PNAS web site). According to this structural gating mechanism, the Cys-loop and 2-3L region are critically positioned at a pivot point between the ACh-binding site and the ion channel (Fig. 3*d* and Fig. 8, which is published as supporting information on the PNAS web site).

Finally, a natural mutation that causes severe myasthenia was recently found within the Cys-loop in the nAChR α -subunit (34). The mutation, homologous to the V131L mutation described in the current work, displayed abnormal kinetics of activation. Therefore, beyond the basic understanding of the molecular details of fast activation processes of LGICs, the identified region may be viewed as a potential target for new therapeutic agents that could act as allosteric modulators able to rescue abnormal activation occurring in natural mutants.

We thank B. Molles for critical reading of the manuscript, A. Marty for fruitful discussion on single-channel analysis, H. Betz (Max-Planck-Institute for Brain Research, Frankfurt, Germany) for providing the human $\alpha 1$ GlyR clone, and M. Soudan and Y. Archambeau for technical assistance. This work was supported by the Association Française Contre les Myopathies, the Commission of the European Communities, the Association pour la Recherche Contre le Cancer, the Collège de France, and the Centre National de la Recherche Scientifique.

1. Corringer, P. J., Le Novère, N. & Changeux, J. P. (2000) *Annu. Rev. Pharmacol.* **40**, 431–458.
2. Karlin, A. (2002) *Nat. Rev. Neurosci.* **3**, 102–114.
3. Changeux, J. P. & Edelman, S. J. (2005) *Science* **308**, 1424–1428.
4. Lester, H. A., Dibas, M. I., Dahan, D. S., Leite, J. F. & Dougherty, D. A. (2004) *Trends Neurosci.* **27**, 329–336.
5. Connolly, C. N. & Wafford, K. A. (2004) *Biochem. Soc. Trans.* **32**, 529–534.
6. Absalom, N. L., Lewis, T. M. & Schofield, P. R. (2004) *Exp. Physiol.* **89**, 145–153.
7. Chakrapani, S. & Auerbach, A. (2005) *Proc. Natl. Acad. Sci. USA* **102**, 87–92.
8. Engel, A. G., Ohno, K. & Sine, S. M. (2003) *Nat. Rev. Neurosci.* **4**, 339–352.
9. Laube, B., Maksay, G., Schemm, R. & Betz, H. (2002) *Trends Pharmacol. Sci.* **23**, 519–527.
10. Bertrand, D., Picard, F., Le Hellard, S., Weiland, S., Favre, I., Phillips, H., Bertrand, S., Berkovic, S. F., Malafosse, A. & Mulley, J. (2002) *Epilepsia* **43**, 112–122.
11. Smit, A. B., Syed, N. I., Schaap, D., van Minnen, J., Klumperman, J., Kits, K. S., Lodder, H., van der Schors, R. C., van Elk, R., Sorgedraeger, B., et al. (2001) *Nature* **411**, 261–268.
12. Brejc, K., van Dijk, W. J., Klaassen, R. V., Schuurmans, M., van der Oost, J., Smit, A. B. & Sixma, T. K. (2001) *Nature* **411**, 269–276.
13. Celie, P. H. N., van Rossum-Fikkert, S. E., van Dijk, W. J., Brejc, K., Smit, A. B. & Sixma, T. K. (2004) *Neuron* **41**, 907–914.
14. Unwin, N. (2005) *J. Mol. Biol.* **346**, 967–989.
15. Miyazawa, A., Fujiyoshi, Y. & Unwin, N. (2003) *Nature* **423**, 949–955.
16. Taly, A., Delarue, M., Grutter, T., Nilges, M., Le Novère, N., Corringer, P. J. & Changeux, J. P. (2005) *Biophys. J.* **88**, 3954–3965.
17. Kash, T. L., Jenkins, A., Kelley, J. C., Trudell, J. R. & Harrison, N. L. (2003) *Nature* **421**, 272–275.
18. Grutter, T., Prado de Carvalho, L., Dufresne, V., Taly, A., Fischer, M. & Changeux, J. P. (2005) *C. R. Biol.* **328**, 223–234.
19. Hamill, O. P., Marty, A., Neher, E., Sakmann, B. & Sigworth, F. J. (1981) *Pflügers Arch.* **391**, 85–100.
20. Palma, E., Bertrand, S., Binzoni, T. & Bertrand, D. (1996) *J. Physiol. (London)* **491**, 151–161.
21. Sigworth, F. J. & Sine, S. M. (1987) *Biophys. J.* **52**, 1047–1054.
22. Grutter, T., Prado de Carvalho, L., Le Novère, N., Corringer, P. J., Edelman, S. & Changeux, J. P. (2003) *EMBO J.* **22**, 1990–2003.
23. Eiselé, J. L., Bertrand, S., Galzi, J. L., Devillers-Thiéry, A., Changeux, J. P. & Bertrand, D. (1993) *Nature* **366**, 479–483.
24. Galzi, J. L., Bertrand, S., Corringer, P. J., Changeux, J. P. & Bertrand, D. (1996) *EMBO J.* **15**, 5824–5832.
25. Heidmann, T. & Changeux, J. P. (1980) *Biochem. Biophys. Res. Commun.* **97**, 889–896.
26. Grever, C. (1999) *Biophys. J.* **77**, 727–738.
27. Edelman, S. J., Schaad, O., Henry, E., Bertrand, D. & Changeux, J. P. (1996) *Biol. Cybern.* **75**, 361–379.
28. Sala, F., Mulet, J., Sala, S., Gerber, S. & Criado, M. (2005) *J. Biol. Chem.* **280**, 6642–6647.
29. Absalom, N. L., Lewis, T. M., Kaplan, W., Pierce, K. D. & Schofield, P. R. (2003) *J. Biol. Chem.* **278**, 50151–50157.
30. Schofield, C. M., Jenkins, A. & Harrison, N. L. (2003) *J. Biol. Chem.* **278**, 34079–34083.
31. Schofield, C. M., Trudell, J. R. & Harrison, N. L. (2004) *Biochemistry* **43**, 10058–10063.
32. Bouzat, C., Gumilar, F., Spitzmaul, G., Wang, H. L., Rayes, D., Hansen, S. B., Taylor, P. & Sine, S. M. (2004) *Nature* **430**, 896–900.
33. Law, R. J., Henchman, R. H. & McCammon, J. A. (2005) *Proc. Natl. Acad. Sci. USA* **102**, 6813–6818.
34. Shen, X. M., Ohno, K. J., Tsujino, A., Brengman, J. M., Gingold, M., Sine, S. M. & Engel, A. G. (2003) *J. Clin. Invest.* **111**, 497–505.